

X-ray absorption spectra at the Ca- $L_{2,3}$ -edge calculated within multi-channel multiple scattering theory

Peter Krüger*

LRRS, UMR 5613 Université de Bourgogne - CNRS, B.P. 47870, 21078 Dijon, France

Calogero R. Natoli

INFN Laboratori Nazionali di Frascati, Casella Postale 13, I-00044 Frascati, Italy

(Dated: November 5, 2021)

We report a new theoretical method for X-ray absorption spectroscopy (XAS) in condensed matter which is based on the multi-channel multiple scattering theory of Natoli *et al.* and the eigen-channel R-matrix method. While the highly flexible real-space multiple scattering (RSMS) method guarantees a precise description of the single-electron part of the problem, multiplet-like electron correlation effects between the photo-electron and localized electrons can be taken account for in a configuration interaction scheme. For the case where correlation effects are limited to the absorber atom, a technique for the solution of the equations is devised, which requires only little more computation time than the normal RSMS method for XAS. The new method is described and an application to XAS at the Ca $L_{2,3}$ -edge in bulk Ca, CaO and CaF₂ is presented.

PACS numbers: 71.15.Qe, 78.70.Dm

I. INTRODUCTION

Multiple scattering (MS) theory provides an accurate and flexible scheme for the calculation of unoccupied electronic states which are probed by various synchrotron experiments such as X-ray absorption spectroscopy and resonant elastic and in-elastic X-ray scattering. The standard theory relies on the single-particle picture, that is, it neglects electron correlation effects. This is a great shortcoming, since core-level X-ray spectra are often strongly modified by electron correlation, in particular by the Coulomb and exchange interaction of the valence electrons with the core hole. In transition metal and rare earth systems, this interaction can give rise to pronounced atomic multiplet and satellite structures in the spectra, which can only be accounted for through many-electron calculations. A generalization of MS theory to many-electron wave functions was developed by Natoli *et al.* [1] and is known as “multi-channel” MS theory. Probably the most difficult part of this approach is the calculation of the inter-channel potential. Here, we propose a reformulation of the theory, where the latter problem is completely avoided. Instead, the multi-channel T-matrix is calculated variationally using the eigen-channel R-matrix method [2, 3, 4, 5, 6]. While R-matrix methods are well known in atomic spectroscopy, they have, to our knowledge, never been used for condensed matter problems. Michiels *et al.* [7] presented a calculation of electron energy loss from NiO using an R-matrix method. They used, however, an atomic model where all solid state effects were described phenomenologically using an crystal field and a reduced Coulomb interaction.

Here, we present a new formalism for X-ray absorption

in condensed matter, based on multi-channel MS theory and the eigen-channel R-matrix method. It allows to take account for local electron correlation effects in a multi-channel, that is, configuration interaction scheme. At present, the type of correlations that can be handled on this level are limited to those between one electron in a delocalized state and a finite number of electrons/holes in (sufficiently) localized orbitals. Sufficiently localized means that the wave function is negligible small beyond the atomic radius. This applies exactly to inner-core shells and well to the $4f$ -shell in rare earths. Extensions of the method to include correlation effects between several delocalized electrons are under way.

In this paper, we present the formalism and report results on the Ca- $L_{2,3}$ -edge absorption of different Ca compounds. The Ca- $L_{2,3}$ -edge is an interesting test case for the new method, because the L_2 and L_3 absorption channels are strongly coupled through the photo-electron – core-hole Coulomb interaction. This leads to a branching ratio of about 1:1, far from the statistical ratio (2:1) which is obtained in single-particle theory. From a point of view of atomic multiplet theory [8, 9, 10], the non-statistical branching ratio is easily understood as a case of strong intermediate coupling in the $(2p^5 3d^1)$ final state. The multipole and exchange part of the $2p$ - $3d$ Coulomb interaction (Slater-integrals F^k , G^k with $k > 0$) is of comparable strength as the $2p$ -spin-orbit interaction, which gives rise to correlated $2p^5 3d^1$ final state wave functions, where the $2p_{1/2}$ and $2p_{3/2}$ -holes are strongly mixed. The fact that the branching ratio does not change when going from atomic Ca [8] to various Ca compounds [11] is empirical evidence that this atomic multiplet picture remains valid in condensed matter. However, a purely atomic model is not sufficient to account for fine structure in the $L_{2,3}$ -edge spectra, which depends strongly on the atomic environment [11] (and which is thereby of practical importance for structural

*Electronic address: pkruger@u-bourgogne.fr

and electronic analysis.) Atomic models including crystal field have proved quite successful in reproducing the experimental spectra at the $L_{2,3}$ -edge [10, 11]. In that approach, all extra-atomic effects are, however, treated in an empirical way, by introducing adjustable parameters for crystal field and (possibly) band broadening. Zaanen *et al.* [9] was the first to go beyond the atomic model by considering a model Hamiltonian that included not only the atomic $2p$ - $3d$ multiplet coupling but also the single electron density of states of bulk Ca. The electron-hole problem was solved exactly using a Green's function technique. While being physically sound, Zaanen's method was not fully based on first principle calculations, but introduced a number of empirical parameters. Later on, Schwitalla and Ebert [12] calculated the spectra in the time-dependent local-density-approximation (TD-LDA). For bulk Ca, they obtained the correct branching ratio, but the fine structure of their spectrum was quite different from the experimental one. Recently, Ankudinov *et al.* [13] studied the branching ratio problem with a generalization of TD-LDA. By adding a frequency and matrix-element dependent exchange-correlation contribution to the TD-LDA kernel, they obtained a branching ratio in good agreement with experiment for Ca and the whole transition metal series, while in Ref. [12] this was true only for the lighter elements (from Ca to V). From the theoretical studies cited above, it may seem that the branching ratio problem at the $L_{2,3}$ -edge of Ca has been thoroughly investigated. Despite of this, we have chosen the Ca system as a test case for our new method, which, we believe, provides new insight into other aspects of the problem, like the orbital relaxation around the core-hole and the reason for the need of a 20% reduction of the Slater integrals F^k and G^k in atomic multiplet calculations [10]. The novelty of the present method comes in at two levels: it is the first application of the multi-channel MS formalism and it is (to our knowledge) the first true application of R -matrix techniques to a condensed matter problem. The combination of these two features will allow us to shed some light on the two points mentioned above (orbital relaxation and reduction factors) and to present an application to the Ca compounds CaO and CaF₂, in which ligand field effects and multiplet structure are treated in a unique framework in an *ab initio* way.

The paper is organized as follows. In section II, the more general aspects of the formalism are outlined. Further details about the multi-channel MS theory can be found in the appendix. In section III the formalism is applied to the $L_{2,3}$ -edge absorption of $3d^0$ systems with an emphasis on the screened electron-hole interaction in the final state. In section IV some numerical aspects are discussed. In section V results are presented for bulk Ca, CaO and CaF₂. Finally, some conclusions are drawn in section VI.

II. GENERAL FORMALISM

In the present approach we go beyond the independent particle model by considering a correlated wave function for a finite number of N electrons. All other electrons are described within the independent particle approximation. Among the N explicitly treated electrons, at most one is in a delocalized orbital, all others necessarily occupy localized orbitals. By definition, a localized orbital is one that is negligibly small outside the atomic sphere. This applies exactly to inner shell orbitals but also to a good approximation to $4f$ -orbitals of the rare-earths. In the ground state wave function, the N electrons include the core electron that is excited in the XAS process plus $N - 1$ other electrons in localized orbitals. The XAS final state wave function then contains $N - 1$ localized electrons and one electron (the "photo-electron") in a delocalized state above the Fermi level. In other words, we consider a correlated final state wave function that couples the photo-electron with the core-hole and and/or a finite number of other localized electrons.

In order to make the derivation less abstract, we shall now consider the specific case of XAS at the Ca- $L_{2,3}$ edges. The formulae are kept general and can easily be applied to other systems to be described with correlated wave functions satisfying the above requirements. For the ground state we consider the six electron wave function made of the $2p$ core electrons. The initial state Ψ_g with energy E_g is thus simply given by the closed shell configuration ($2p^6, {}^1S_0$). Final states have energy $E = E_g + \hbar\omega$ and a ($2p^5\epsilon^1$) configuration, where ϵ denotes a (one-electron) state in the continuum above the Fermi energy. The crucial point is that we take into account multiplet effects through a configuration interaction ansatz for the final state wave function, which is developed as

$$\Psi = \mathcal{A} \sum_{\alpha} \tilde{\Phi}_{\alpha}(X) \phi_{\alpha}(x). \quad (1)$$

Here $\tilde{\Phi}_{\alpha}$ is one of the six ($2p^5$) states, labeled by $\alpha = (j_c, \mu_c)$ ($j_c = 1/2, 3/2$, $\mu_c = -j_c \dots j_c$); X collects all core-electron coordinates. The ($2p^5$) multiplet energies are $E_{\alpha} = E_g - \epsilon_c(j_c)$, where $\epsilon_c(j_c)$ are the negative binding energies of spin-orbit split $2p(j_c)$ levels. For each $\tilde{\Phi}_{\alpha}$, there is a component ϕ_{α} of the photo-electron wave function. The (radial, angular, and spin) coordinate of the photo-electron is denoted $x = (r, \hat{x}, \sigma)$. Finally, \mathcal{A} denotes the anti-symmetrization operator.

Multi-channel multiple scattering. The total photo-absorption cross section is calculated using the multi-channel multiple scattering method by Natoli *et al.* [1]. As shown in detail in the appendix, it is given by

$$\sigma(\omega) \propto \omega \text{Im} \left\{ \sum_{\Gamma\Gamma'} M_{\Gamma}^* \tau_{\Gamma\Gamma'}^{00} M_{\Gamma'} \right\}. \quad (2)$$

Here $\Gamma = \alpha L s$ is the set of all quantum numbers of Ψ , with $L \equiv lm$ being the orbital and s the spin quantum

numbers of the photo-electron. $M_\Gamma = \langle \Psi_\Gamma^{\text{in}} | D | \Psi_g \rangle$ are the transition matrix elements; we consider only dipole transition in the length approximation. Ψ_Γ^{in} is the inside solution that matches smoothly onto the outside solution

$$\Psi_\Gamma^{\text{out}} = \sum_{\Gamma'} \Phi_{\Gamma'}(X\hat{x}\sigma) Z_{\Gamma'\Gamma}(r)/r. \quad (3)$$

Here, we have introduced $\Phi_\Gamma \equiv \tilde{\Phi}_\alpha(X) Y_L(\hat{x}) \delta_{s,\sigma}$. “Inside” and “outside” refer to the atomic sphere of the absorber, i.e. $r < r_0$ and $r > r_0$, respectively, r_0 being the muffin-tin radius. The matrix Z of radial photo-electron functions is given by

$$Z_{\Gamma\Gamma'}(r)/r = j_l(k_\alpha r)[t_0^{-1}]_{\Gamma\Gamma'} - ik_\alpha h_l^+(k_\alpha r) \delta_{\Gamma\Gamma'}. \quad (4)$$

Here, $h_l^+ = j_l + in_l$ and j_l, n_l are the usual spherical Bessel and Neumann functions. k_α is the wave number of the photo-electron, given by $k_\alpha^2 + V_0 = \epsilon_\alpha = E - E_\alpha$, where V_0 is the interstitial potential. $t_{\Gamma\Gamma'}$ is the multi-channel atomic T-matrix of the absorber (at site $i=0$). In Eq. (2), $\tau_{\Gamma\Gamma'}^{ij}$ is the multi-channel scattering path operator connecting sites i and j . It is calculated for a finite cluster by inversion of the matrix $m \equiv \tau^{-1}$, whose elements are given by

$$m_{\Gamma\Gamma'}^{ij} = \delta_{ij}[t_i^{-1}]_{\Gamma\Gamma'} - \delta_{\alpha\alpha'} k_\alpha G_{LL'}^{ij}(k_\alpha) \delta_{ss'}. \quad (5)$$

Here, t_i is the multi-channel atomic scattering matrix of atom i , and $G_{LL'}^{ij}$ are the real space KKR structure factors.[14] Apart from the absorber, we treat all atoms in the standard one-electron muffin-tin approximation, which implies $t_{i,\Gamma\Gamma'} = t_{il}(k_\alpha) \delta_{\Gamma\Gamma'}$, for all $i \neq 0$. Since these T-matrices for $i \neq 0$ as well as the structure factors $G_{LL'}^{ij}$ are single-channel quantities, the only channel-off-diagonal terms of m are located in $i=j=0$ block. This particular structure of the m -matrix allows us to use an efficient partitioning technique for the inversion of m .

Partitioning technique. We divide the system into absorber atom ($i=0$) and “environment”, i.e. all other atoms with $i \neq 0$, collectively labeled ‘ e ’. For the absorption cross section we need only the absorber block τ^{00} of the τ -matrix. Using simple matrix algebra, this quantity can be expressed as

$$\tau^{00} = (m^{00} - m^{0e}[m^{ee}]^{-1}m^{e0})^{-1} = (t_0^{-1} - \rho)^{-1} \quad (6)$$

In the second equality, we have used $m^{00} = t_0^{-1}$ and introduced the reflectivity $\rho \equiv m^{0e}[m^{ee}]^{-1}m^{e0}$, which contains all the information we need from the environment. Once ρ is known, the remaining problem is a purely atomic one. Now ρ is diagonal in the channel indices α since it does not involve the $i=j=0$ block of the m -matrix. It can therefore be calculated using standard (single-channel) MS theory. Explicitly, we have

$$\rho_{\Gamma\Gamma'} = \delta_{\alpha\alpha'} \rho_{LL'}(k_\alpha) \delta_{ss'}, \quad (7)$$

where

$$\rho_{LL'}(k) = k^2 \sum G_{LL''}^{0i}(k) \tilde{\tau}_{L''L'''}^{ij}(k) G_{L''L'}^{j0}(k). \quad (8)$$

Here, the sum runs over $L'', L''', i \neq 0, j \neq 0$, and $\tilde{\tau}$ is the single-channel τ -matrix of the system without absorber (α -diagonal terms of $[m^{ee}]^{-1}$).

Eigen-channel R-matrix method. The remaining problem is the calculation of the multi-channel T-matrix of the absorber and the inner solutions Ψ_Γ^{in} . This is done using the eigen-channel R-matrix method [2, 3, 4, 5, 6]. In the following we recall some basic features of this method for the convenience of the reader and in order to introduce our notation (which follows most closely that of Ref. [5]). The R-matrix is a multi-channel generalization of the logarithmic derivative of the radial wave function. As reaction volume, we use the atomic (or “muffin-tin”) sphere of the absorbing atom with radius r_0 . With Eq. (3), the R-matrix can be defined as

$$\sum_{\Gamma''} R_{\Gamma\Gamma''} \dot{Z}_{\Gamma''\Gamma'}(r_0) = Z_{\Gamma\Gamma'}(r_0). \quad (9)$$

Here we have introduced the notation $\dot{X} \equiv dX/dr$. Using Eq. (4) and its derivative with respect to r , the t -matrix can be readily calculated from the R-matrix as

$$t^{-1} = iK(RJ - J)^{-1}(R\dot{H} - H). \quad (10)$$

Here all the quantities are matrices with indices $\Gamma\Gamma'$ and are evaluated at $r = r_0$. Furthermore, the quantities K, J, H are diagonal matrices with elements $K_{\Gamma\Gamma} = k_\alpha$, $J_{\Gamma\Gamma} = k_\alpha r_0 j_l(k_\alpha r_0)$, and $H_{\Gamma\Gamma} = k_\alpha r_0 h_l^+(k_\alpha r_0)$.

In the eigen-channel method, the R-matrix is obtained directly in diagonal form; for given energy E , a basis of eigenstates Ψ_k and eigenvalues b_k is found, by solving the following generalized eigenvalue problem [5, 6].

$$(E - H - L)\Psi_k = Q\Psi_k b_k. \quad (11)$$

Here H is the Hamiltonian, $L \equiv \sum_{i=1}^N \delta(r_i - r_0) \frac{1}{r_i} \frac{\partial}{\partial r_i} r_i$ is the Bloch operator that restores Hermiticity of H in the finite reaction volume, i.e. the atomic sphere and $Q \equiv \sum_{i=1}^N \delta(r_i - r_0)$ projects onto its surface. Among all solutions of Eq. (11), only those with $|b_k| < \infty$ are physically acceptable. Their number equals the number of channels Γ [4]. In order to solve Eq. (11) we develop

$$\Psi_k = \sum_{\Gamma\nu} \Psi_{\Gamma\nu} c_{\Gamma\nu,k} \quad (12)$$

with trial functions of the form

$$\Psi_{\Gamma\nu} \equiv \mathcal{A} \{ \Phi_\Gamma(X\hat{x}\sigma) P_\nu(r)/r \}. \quad (13)$$

As radial basis functions P_ν , we use solutions of the radial Schrödinger equation for angular momentum l and a spherically symmetric, local one-electron potential $v_{\text{eff}}(r)$. In the present application, we take for v_{eff} the sum of the ground state potential v_g and a partially screened core-hole potential v_c (see Eq. (16) below). As usual in the eigen-channel method, we use closed-type orbitals with boundary conditions $P_\nu(r_0) = 0$, and open-type orbitals with boundary conditions $dP_\nu/dr(r_0) =$

0. Since $2p \rightarrow \epsilon s$ transitions have negligible intensity in the near-edge region, we here include only $l = 2$, i.e. d -waves in the basis. The generalized eigenvalue problem in Eq. (11) is solved using standard numerical routines [15]. The eigenvectors of the R-matrix are given by $W_{\Gamma k} \equiv \sqrt{N} r_0 \int \Phi_{\Gamma} \Psi_k$, where the integration is over $X\hat{x}\sigma$ and the remaining radial coordinate of Ψ_k is taken at r_0 [5]. The factor \sqrt{N} comes from antisymmetrization. From the orthogonality of the channel functions Φ_{Γ} and Eqs (12,13) we have

$$W_{\Gamma k} = \sum_{\nu} c_{\Gamma\nu,k} P_{\nu}(r_0) .$$

We normalize the generalized eigenvectors $c_{\Gamma\nu,k}$ (k fixed) such that $\sum_{\Gamma} |W_{\Gamma k}|^2 = 1$. Then W is unitarian and the R-matrix is given by

$$R_{\Gamma\Gamma'} = - \sum_k W_{\Gamma k} b_k^{-1} W_{k\Gamma'}^{\dagger} .$$

The inner solutions that match the outer ones are

$$\Psi_{\Gamma}^{\text{in}} = \sum_{\Gamma'\Gamma''\nu k} \Psi_{\Gamma'\nu} c_{\Gamma'\nu,k} W_{k\Gamma''}^{\dagger} Z_{\Gamma''\Gamma}(r_0) .$$

III. ELECTRON-HOLE INTERACTION

We describe the sub-system of N electrons through a Hamiltonian of the form

$$H^{(N)} = H_0 + V = \sum_{i=1}^N h_0(i) + V .$$

Here h_0 is the one particle Hamiltonian of the chosen independent electron model and i is an electron label. If N was the number of all electrons in the system (N_{all}), the exact perturbation V would be given by the bare two-particle electron-electron interaction terms minus the effective electron-electron potential v_{eff} that is included in h_0 . However, since in our case $N \neq N_{\text{all}}$, there is no (simple) exact expression of $H^{(N)}$ and the “best” approximation for V is not necessarily given by the exact expression of the case $N = N_{\text{all}}$. The reason is that v_{eff} and thus h_0 are determined by N_{all} rather than only N electrons, and the Coulomb interaction in V is screened by the $N_{\text{all}} - N$ other electrons.

For the system studied here, these considerations are of interest only for the final state. The ground state, being a closed shell configuration ($2p^6, ^1S$), is well described by a single Slater determinant with the ($2p$) orbitals calculated from h_0 . For the ($2p^5\epsilon^1$) final states, the perturbation V is the screened photo-electron – core-hole Coulomb interaction.

We shall first take for V the unscreened interaction and discuss the effect of screening below. We have to calculate the matrix elements of H , L and Q for the basis states

in Eq. (13), which we denote as $|\Gamma\nu\rangle \equiv |2p^5\nu d^1, \Gamma\rangle$ with $\Gamma=j_c\mu_c ms$. We have

$$\langle \Gamma\nu | H_0 | \Gamma'\nu' \rangle = (E_g - \epsilon_c(j_c) + \epsilon_{\nu}) \delta_{\Gamma\Gamma'} S_{\nu\nu'} ,$$

where

$$S_{\nu\nu'} \equiv \int_0^{r_0} dr P_{\nu}(r) P_{\nu'}(r)$$

is the overlap integral, ϵ_{ν} is the energy of the P_{ν} orbital, and the other quantities have been defined before. Note that $\delta_{\Gamma\Gamma'}$ is ensured by the orthogonality of the angular and spin functions. For the calculation of the matrix elements of V , we make a basis transformation from the uncoupled states $|2p^5 j_c \mu_c, \nu d^1 ms\rangle$ to LS coupled states $|2p^5 \nu d^1, (LS)JM\rangle$ [16]. In the LS coupled basis, the matrix elements of V are given by

$$\langle \Gamma\nu | V | \Gamma'\nu' \rangle = [w(^{2S+1}L)]_{\nu\nu'} \delta_{\Gamma\Gamma'} , \quad (14)$$

where now $\Gamma=(LS)JM$. The w 's can be expressed in terms of the following generalized Slater integrals

$$F_{\nu\nu'}^k \equiv \int_0^{r_0} dr \int_0^{r_0} dr' P_{2p}(r) P_{\nu}(r') \frac{2r_{<}^k}{r_{>}^{k+1}} P_{2p}(r) P_{\nu'}(r') ,$$

$$G_{\nu\nu'}^k \equiv \int_0^{r_0} dr \int_0^{r_0} dr' P_{2p}(r) P_{\nu}(r') \frac{2r_{<}^k}{r_{>}^{k+1}} P_{\nu'}(r) P_{2p}(r') .$$

Here, $r_{>(<)}$ is the larger (smaller) of r and r' . The expressions for the $w(^{2S+1}L)$ are given in Ref. [17]:

$$\begin{aligned} w(^1P) &= -F^0 - F^2/5 + 4G^1/49 \\ w(^3P) &= -F^0 - F^2/5 \\ w(^1,^3D) &= -F^0 + F^2/5 \\ w(^1F) &= -F^0 - 2F^2/35 + 18G^3/49 \\ w(^3F) &= -F^0 - 2F^2/35 \end{aligned}$$

where, in our case, all quantities are matrices with indices $(\nu\nu')$. The matrix elements of the other operators needed in the eigen-channel method are easily calculated:

$$\langle \Gamma\nu | E | \Gamma'\nu' \rangle = E \delta_{\Gamma\Gamma'} S_{\nu\nu'} ,$$

$$\langle \Gamma\nu | Q | \Gamma'\nu' \rangle = \delta_{\Gamma\Gamma'} P_{\nu}(r_0) P_{\nu'}(r_0) ,$$

$$\langle \Gamma\nu | L | \Gamma'\nu' \rangle = \delta_{\Gamma\Gamma'} P_{\nu}(r_0) \frac{P_{\nu'}}{dr}(r_0) .$$

The dipole operator selects (1P) basis states and thus only $J = 1$ final states give a contribution. The reduced matrix elements are non-zero for $\Gamma=(^2S+1)L_1, M=1$ and given by

$$\langle \Psi_g || r || \Psi_{\Gamma}^{\text{in}} \rangle = -2 \sum_{\nu k \Gamma'} I_{2p, \nu} c_{\Gamma_0 \nu}^{(k)} W_{k\Gamma'}^{\dagger} Z_{\Gamma'\Gamma}(r_0) \quad (15)$$

with $\Gamma_0=(^1P_1, M=1)$ and $I_{2p, \nu} = \int_0^{r_0} P_{2p}(r) r P_{\nu}(r) dr$.

Screening model. As it is well known from cluster and impurity model calculations [9], the monopole term of the electron-hole Coulomb interaction (corresponding to the Slater integral F^0) is drastically screened, while the higher order multipole and all exchange terms (Slater integrals F^k , G^k with $k > 0$) are essentially unscreened. Let us note that in multiplet calculations also the higher order terms are generally reduced from the calculated values.[9, 10] The need for this reduction of some 20% is, however, not due to screening, but comes mainly from the neglect of configuration interaction in the single-configuration multiplet approach [18]. As will become apparent in the next section, the relevant configuration interaction is included in our approach, so that there is no need for reduction of the Slater integrals with $k > 0$.

We therefore apply screening only to the monopole term $2/r_{>}$ of the Coulomb operator $2/|\mathbf{x} - \mathbf{x}'|$. This defines the (unscreened) multipole part $\tilde{V} \equiv 2/|\mathbf{x} - \mathbf{x}'| - 2/r_{>}$ of the interaction V . In the space of trial functions $\Psi_{\Gamma\nu}$ we have chosen, the operator $2/r_{>}$ is diagonal in Γ . Within this space, it is therefore equivalent to a one-electron potential $v_u(r)$, namely the Hartree potential of a spherically symmetric core-hole which is given by : $v_u(r) = \int dr' [P_{2p}(r')]^2 / r_{>}$. We can thus handle screening of the monopole term on a single-particle level by replacing the unscreened core-hole potential $v_u(r)$ by a screened one $v_c(r)$, which we add to h_0 . In this way the effective potential v_{eff} used in h_0 will not be the ground state self-consistent potential v_g but $v_{\text{eff}} = v_g + v_c$.

A simple approximation for v_{eff} is given by the fully statically screened potential $v_{\text{supercell}}$ which is obtained from a self-consistent super-cell calculation with a core-hole on the absorber site. This effective potential, which features full orbital relaxation around the core-hole, is frequently used in single-electron XAS calculations. We shall denote the corresponding core-hole contribution by v_s , i.e. $v_s \equiv v_{\text{supercell}} - v_g$. As will become apparent in the result section below, the line shapes obtained with v_s are not satisfactory. We shall therefore allow for incomplete screening by using a linear mixture between the unscreened core-hole potential v_u and the fully screened one v_s :

$$v_c(r) = \alpha v_u(r) + (1 - \alpha) v_s(r) , \quad (16)$$

where $\alpha \in [0, 1]$ is an empirical parameter. As can be seen from the results below, a value of $\alpha \approx 0.1$ gives best agreement with experiment. This fact indicates that orbital relaxation around the core-hole is overestimated in $v_{\text{supercell}}$ which, we recall, is obtained from a super-cell calculation in the *local density approximation* (LDA). This finding was to be expected, since it is known that in LDA the self-interaction of an electron is not exactly compensated as in the Hartree-Fock scheme, giving rise to over-relaxation and band gaps that are systematically too small compared to experiment. Probably the same calculation with Self-Interaction Corrections would cure this drawback. This will be the subject of a future investigation. In the meantime we regard α as useful pa-

rameter describing the correct amount of relaxation. Let us also note that an *a priori* estimate of this quantity could be obtained in a multi-channel MS theory that starts from the fully relaxed state and mixes in very many charge transfer excitations. This possibility shall also be explored in the future.

In summary, the present treatment of screening consists in (i) replacing the screened electron-hole Coulomb interaction V by its unscreened multipole part $\tilde{V} = 2/|\mathbf{x} - \mathbf{x}'| - 2/r_{>}$ and (ii) adding the partially screened core-hole potential $v_c(r)$ in Eq. (16) to the single-particle Hamiltonian h_0 . Point (ii) results in a modification of all radial wave functions $P_\nu(r)$ and corresponding energies ϵ_ν , whereas point (i) simply removes all monopole terms ($F_{\nu\nu'}^0$) from the interaction matrix (14).

IV. NUMERICAL ASPECTS

The standard MS calculation for the reflectivity of the environment $\rho_{LL'}(k)$ has been performed using the CONTINUUM code [19]. Finite clusters containing at least nine nearest neighbor shells around the absorber were used for all systems, such that the XAS spectra were well converged with respect to cluster size. The effective single-particle potential was calculated self-consistently in the local density approximation using the linear-muffin-tin-orbital method [20]. In all systems we used space-filling (and thus partially overlapping) atomic spheres. In the compounds CaO and CaF₂, we chose the relative atomic radii in such a way that the potential value on the sphere was approximately equal for Ca and the ligand, while keeping the overlap volume small. For CaO, a ratio of 3:2 between the Ca and O radii was found appropriate. For CaF₂, the insertion of one empty sphere (E) per formula unit was necessary to keep the overlap small. We chose the ratio of the sphere radii of Ca:O:E to be 6:4:5, approximately. The fully screened core-hole potential v_s was obtained from super-cell calculations with a (spherically symmetric) $2p$ -hole on the absorber atom. We used a 32 atom simple cubic super-cell for Ca metal, and an fcc $2 \times 2 \times 2$ super-cell for CaO and CaF₂. We found that the core-hole has only a small effect on the potentials of the *neighboring* atoms and that, consequently, it makes hardly a difference for the spectra whether the reflectivity is calculated with or without the core-hole potential. On the absorber atom, however, $v_c(r)$ is strong and has a dramatic effect on the line shape as will become apparent below.

For reasons of numerical stability, the reflectivity was calculated at complex energies with a small imaginary part, such that the spectra are effectively broadened with a Lorentzian function of about 0.3 eV FWHM. In order to simulate finite experimental resolution, the spectra in the *result section* were further broadened with a Gaussian function of 0.3 eV FWHM.

In the eigen-channel method, convergence with respect to the number of radial basis functions has to be achieved.

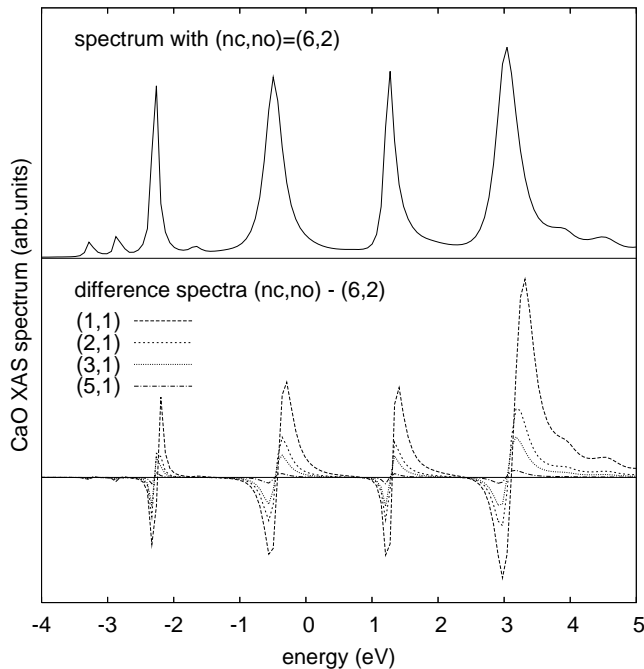


FIG. 1: Convergence of the spectra with respect to the number of radial basis functions in the example of CaO. The numbers of closed-type (nc) and open-type (no) basis functions are indicated as (nc,no) .

In Fig. 1 we show this convergence in the example of CaO. The different basis sets are indicated as (nc,no) , where nc (no) is the number of closed-type (open-type) functions. We start from functions without nodes in $0 < r < r_0$ and increase the number of nodes one by one. For example, the (3,1) spectrum was obtained with three closed type functions of zero, one and two nodes and one open-type function of zero nodes. Figure 1 shows the converged spectrum with basis set (6,2) in the upper panel and difference spectra with respect to (6,2) in the lower panel. It can be seen that five closed-type and only one open-type function are sufficient for good convergence. For the spectra in the results section below, we have used the (5,1) basis set.

It is interesting to note that one can considerably improve the spectrum calculated with the minimal (1,1) basis set by reducing the values of the Slater integrals F^k , G^k (artificially) by some 20%. Figure 2 shows the (1,1) spectrum with full (a) and 20% reduced (b) values of the Slater integrals, along with the converged spectrum (c), which was multiplied by 1.4 for easy comparison of the peak ratios. Clearly, a 20% reduction of Slater integrals improves considerably the (1,1) line shape, both as far as peak positions and relative peak intensities are concerned. Apart from the overall amplitude, which is about 40% too big, the spectrum almost coincides with the converged one. This result is closely related to the fact that in atomic single configuration multiplet calculations, reduction factors of 10-25% for the Slater integrals

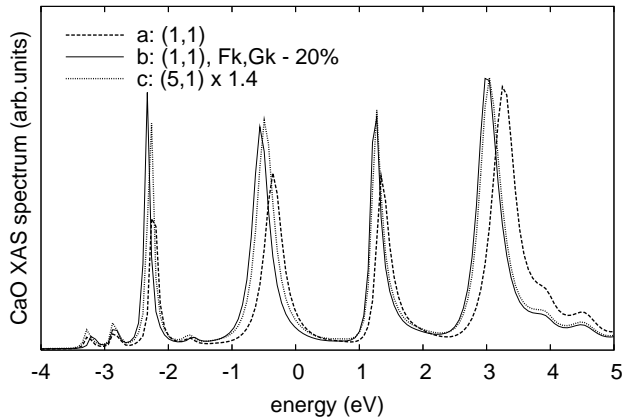


FIG. 2: CaO spectra obtained with the minimal basis set $(nc,no)=(1,1)$, along with the converged one (c). The latter was multiplied by a factor 1.4 for easy comparison. Spectrum (b) was calculated with the Slater integrals F^k , G^k reduced by 20%.

are generally needed to make the relative multiplet energies and line strengths agree with experiment [10, 18]. Such a rescaling procedure effectively accounts for configuration interaction that lies beyond the single configuration calculation [18], namely coupling to higher lying electronic configurations. Precisely this feature is seen in Fig. 2, when one realizes that in the minimal set (1,1) describes essentially only the 3d orbital, while in the (5,1) basis set of the converged spectrum, all nd orbitals up to $n = 7$ are included.

In the practical implementation of the method, we first calculate the reflectivity matrix $\rho_{LL'}(k)$ on a fine mesh in the relevant (photo-electron) energy interval. In a second step the atomic multichannel calculation is performed for each total energy $E = E_g + \omega$. The R-matrix and the inner solutions $\Psi_{\Gamma}^{\text{in}}$ are calculated through the eigenchannel method and then the atomic multi-channel T-matrix t_0 and the dipole transition matrix elements are readily obtained from Eqs (10) and (15). We get the reflectivity $\rho_{LL'}(k_{\alpha})$ at the photo-electron energies k_{α} of the different channels α , needed in Eq. (7) by interpolation in k . Finally, we invert the matrix $t_0^{-1} - \rho$ (Eq. 6) and obtain the XAS cross section from Eq. (2).

By virtue of the separation between environment and absorber through the partitioning technique, the present implementation of the multi-channel MS method is numerically only little heavier than the standard (single-channel) MS method. Indeed, in the present application, the atomic multi-channel calculation (second step above) was an order of magnitude faster than the reflectivity calculation by the standard MS technique.

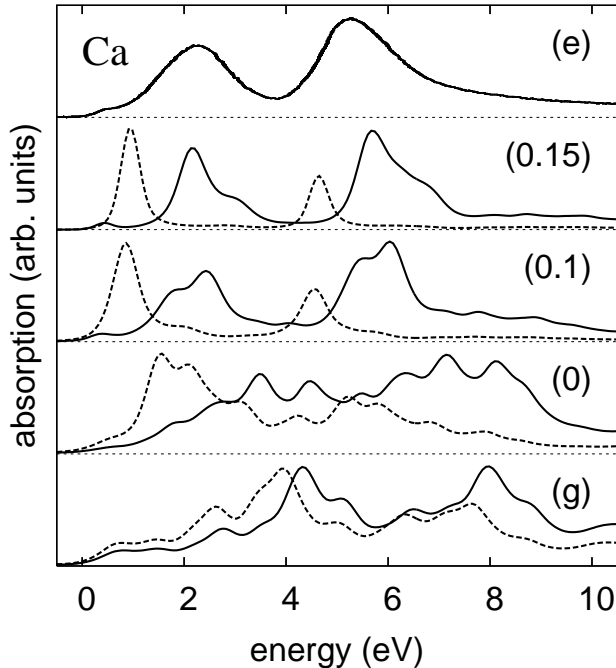


FIG. 3: X-ray absorption spectra at the Ca- $L_{2,3}$ -edge in bulk Ca. Curve (e) is the experimental spectrum taken from Ref. [11]. In the theoretical spectra, (g) was obtained from the ground state potential, and the others with a (partially) screened potential with the screening factor indicated as (α). In all cases, the one-electron spectrum (without \tilde{V}) is shown with a dashed line and the multi-channel calculation (including \tilde{V}) with a full line.

V. RESULTS FOR THE Ca $L_{2,3}$ -EDGE

Figure 3 shows the $L_{2,3}$ -edge absorption of bulk Ca calculated in different approximations, along with the experimental spectrum (e) taken from Ref. [11]. The numbers in parenthesis indicate the value of the screening parameter α of the core-hole potential v_c in Eq. (16). The spectra labeled (g) have been obtained with the ground state potential (i.e. $v_c = 0$). The spectra in full (dashed) lines have been calculated with (without) the multipole part of the electron-hole interaction \tilde{V} . For easy comparison of the line shapes, all spectra are aligned at threshold and normalized with respect to the height of their main peak. Note that before normalization, the intensity of the spectra without \tilde{V} (dashed lines) was considerably bigger than the corresponding spectra with \tilde{V} (full lines). The relative renormalization factors between the two types of spectra, that have been used in Fig. 3, are: 1.8 (g), 2.3 (0), 3.3 (0.1), and 3.8 (0.15).

Probably the most striking feature of the spectra in Fig. 3 is the effect of the multipole part of the electron-hole interaction \tilde{V} : in all cases, it leads to a big transfer of spectral weight from the L_3 edge (lower energy peak) to the L_2 -edge. The branching ratio thus changes from

2 : 1 without \tilde{V} to somewhat less than 1 : 1, which is in good agreement with experiment. This spectral weight transfer comes from the mixing between the $2p_{1/2}$ and the $2p_{3/2}$ -hole states (which correspond, in the one-electron approximation, to the L_2 and L_3 edges, respectively). It is a genuine atomic multiplet effect which was first explained by Zaanen *et al.* [9]. As can be seen from a “vertical” comparison in Fig. 3, the choice of the core-hole potential v_c has only a minor effect on the branching ratio, but it changes the line shape of the two edges *individually*, as it can be expected from a single-particle quantity. Going from (g) to (0), or increasing the parameter α has the effect of shifting the peak positions of the two edges to lower energy and of reducing their width. It moreover leads an overall shift of the whole spectrum to lower energy. This shift, which is roughly 1 eV for (g) \rightarrow (0), (0) \rightarrow (0.1), and (0.1) \rightarrow (0.15), is, however, not apparent from Fig. 3, because we have aligned the spectra at threshold. When comparing the spectra including \tilde{V} with the experimental one, it is clear that (g) and (0) have much too broad peaks. Moreover, their peak positions relative to threshold are at too high energy, especially for (g). Good agreement for both peak width and positions is obtained for spectra (0.1) and (0.15). The only disagreement is that these two theoretical spectra show a weak fine-structure which was not observed experimentally. A possible explanation for this discrepancy is the presence of further broadening mechanisms, other than coupling to the band, which is included here by the multiple scattering of the photo-electron. Himpsel *et al.* suggested that the broadening might be due to strong auto-ionization. The discrepancy could, however, also reveal limitations of the present screening model, which neglects charge fluctuations. Let us note that our spectrum (g) looks identical with the one obtained by Schwitalla *et al.* [12] within time-dependent local density approximation. This shows that their method does not take account of the monopole part of the electron-hole interaction.

For a contrast to the *metallic* bulk Ca, we have applied the method also to two *insulating* Ca compounds: CaO and CaF₂. The results are shown in Fig. 4. As in Fig. 3, the spectra have been normalized and aligned at threshold. For the latter, the spectra (g) have been shifted by 3.5 eV to lower energy relative to the others in both compounds. The meaning of labels and line-styles is the same as in Fig. 3. The spectra (g), which correspond to a total neglect of the core-hole and the multipole terms \tilde{V} , are again completely at odds with the experimental spectrum (e). When using a screened core-hole potential v_c with $\alpha = 0.1$, but still neglecting the multipole terms \tilde{V} [dashed line (0.1)], the spectra consist of four narrow lines (the finite width comes entirely from the added Lorentzian+Gaussian broadening). The splitting of the L_3 and L_2 peaks into two doublets is due to a strong ligand field effect. By symmetry resolved MS calculations, we have checked that for CaO, the lower (higher) energy peaks correspond to t_{2g} (e_g) symmetry

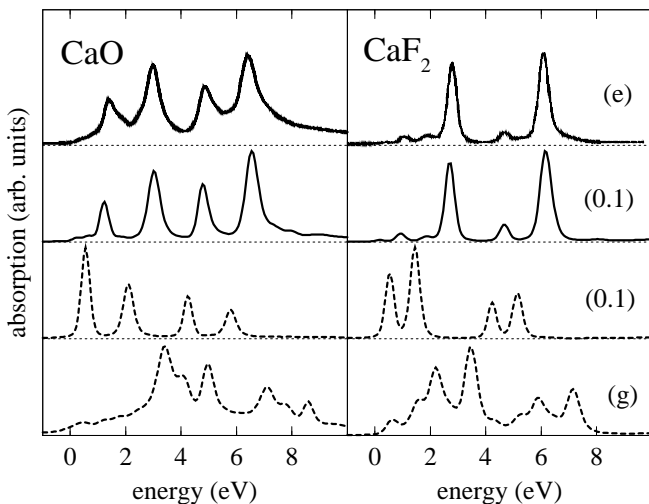


FIG. 4: X-ray absorption spectra at the Ca-L_{2,3}-edge in CaO and CaF₂. Labels and line-styles have the same meaning as in Fig. 3, i.e. (e) experiment, (g) ground state potential, (0.1) v_c with $\alpha=0.1$. A full (dashed) line corresponds to a calculation with (without) \tilde{V} .

states in the O_h point group. In CaF₂ the order between t_{2g} and e_g peaks is reversed. These spectra are, however, still very different from the experimental ones. When finally also the multipole part of the interaction \tilde{V} is taken into account [full line (0.1)], very good agreement with experiment is obtained for both compounds. It should be noted that Himpsel *et al.* [11], who used an atomic crystal field model, could also get very good agreement with experiment. However, in that work the crystal field is introduced empirically and its parameter values are adjusted to experiment.

VI. CONCLUSIONS

In summary, we have presented a method for X-ray absorption in condensed matter where single-electron features are described in the MS approach, while local multi-electron effects are taken into account in a configuration interaction scheme. The novel features of the method are the multi-channel extension of MS theory and the use of an R-matrix technique in condensed matter.

The method has been applied to the Ca-L_{2,3} edge absorption of several Ca systems. The electron-hole Coulomb interaction was divided into its monopole and its (higher order) multipole part. The latter, which is responsible for the non-statistical L₃:L₂ branching ratio, was taken unscreened. We showed that no rescaling for this part is needed in our method in contrast to single configuration multiplet calculations. For the monopole term, a mixture between an unscreened and a statically screened core-hole potential was applied. A mixing factor of about 10% yields line shapes in good agreement with experiment in all cases.

Non-local correlation effects such as charge transfer excitations have been neglected in the present work. Let us mention, however, that such effects can, in principle, be included when the R-matrix reaction volume is extended from a single atom to a small cluster of atoms around the absorber. Compared to recent approaches based on time dependent density functional theory [12, 13], we believe that the present, configuration interaction based method provides more insight in the correlation mechanisms at play. Moreover, the present approach can easily be applied to problems where the applicability of TD-DFT has yet to be proved, namely core-level spectroscopies that involve more than one hole (such as Auger processes) or open 4*f*-shells. Compared to atomic multiplet methods [10], the present approach does not rely on adjustable crystal field parameters. Instead, ligand field and band effects are described in an *ab initio* manner through MS theory.

VII. ACKNOWLEDGMENTS

The authors would like to thank K. Hatada for fruitful discussions. P. K. acknowledges financial support from the SRRT network and from INFN.

APPENDIX

Derivation of X-ray absorption cross section formula in multi-channel multiple scattering theory

In this section we derive X-ray absorption cross section formula within the multi-channel multiple scattering method. Most of the results of this section are not new, but can be found as special cases of the more general derivation given in Ref. [1]. Nevertheless, we think it is worth including this section for the convenience of the reader, because the derivation is simpler than the one in Ref. [1] and it lends itself better to the form of the *N*-electron wave functions used in the present work.

We start from the general multi-electron formula for the total optical absorption cross section in the dipole approximation [1]:

$$\sigma = 4\pi^2\alpha\omega \sum_f |\langle \Psi_f | D | \Psi_g \rangle|^2 \delta(E_f - E_g - \omega) \quad (17)$$

Here, Ψ_g and Ψ_f are *N*-electron wave functions, for initial (=ground) and final state, respectively, in the absorption process of a photon with energy ω . In case of degenerate ground states, a sum over *g* is understood. $D \equiv \epsilon \cdot \sum_{i=1}^N \mathbf{x}_i$ is the dipole operator, $\alpha = \frac{1}{137}$ the fine structure constant. We use the units: $\hbar = 1$, Bohr radius for length, Rydberg for energy. Thus $E_{\text{kin}} = k^2$, $e^2 = 2$.

For the ground state, we explicitly take into account only localized electrons of the absorbing atom. Thus we assume that the ground state wave function Ψ_g is

confined to the atomic sphere of the absorber with radius r_0 : $\Psi_g(x_1 \dots x_N) = 0$ if $\exists i : r_i > r_0$. As for the final state wave function Ψ_f , we assume that $N-1$ electrons remain in localized orbitals and at most one electron (the “photo-electron”) is promoted to a continuum orbital. We chose boundary conditions such that in the remote past, the photo-electron is free, i.e. its eigenstates are plane waves $\exp(i\mathbf{k}\mathbf{x})$ times a spin function $\chi_s(\sigma) = \delta_{s\sigma}$. The rest system is in one of the eigenstates $\Phi_\alpha(x_1 \dots x_{N-1})$ of the $N-1$ electron Hamiltonian with a core hole: $H^{N-1}\Phi_\alpha = E_\alpha\Phi_\alpha$. Thus, the “incoming part” of Ψ_f is given by $\Phi_\alpha \times \exp(i\mathbf{k}\mathbf{x})\chi_s(\sigma)$. In multi-channel scattering theory, not only elastic, but also inelastic scattering processes are taken into account, which correspond to excitations $\Phi_\alpha \rightarrow \Phi_\beta$. In the present approach, these excitations are limited to atomic-like ones, such as multiplet excitations, due to the local character of Φ_α . (Note that this is in contrast to the more general theory in Ref. [1]). By expanding the scattered part of Ψ_f over the eigenfunctions Φ_α , we can write

$$\Psi^{(\alpha\mathbf{k}s)} = \Phi_\alpha \exp(i\mathbf{k}\mathbf{x})\chi_s(\sigma) + \sum_\beta \Phi_\beta f_\beta^{(\alpha\mathbf{k}s)}(\mathbf{x}\sigma).$$

Here $f_\beta^{(\alpha\mathbf{k}s)}(\mathbf{x}\sigma)$ behaves asymptotically ($r \rightarrow \infty$) like a purely outgoing spherical wave. In the above form of Ψ_f , anti-symmetrization between the photo-electron and the $N-1$ other electrons has been disregarded. We indeed neglect anti-symmetrization for the “outside solution”, i.e. when the photo-electron is outside the atomic sphere of the absorber. For the solution inside the atomic sphere, however, anti-symmetrization between all electrons is correctly taken into account through the eigen-channel method (see main text). Note that in this work we have, for simplicity, assumed the “muffin-tin” or more precisely atomic sphere approximation for the one-electron potential i.e. the atomic cells are replaced by space filling spheres with spherically symmetric potential inside. The difficulties of multiple-scattering theory arising from non-muffin-tin potentials are essentially independent of the electron correlation problem we are dealing with here. The present multi-channel approach could easily be generalized to non-muffin-tin multiple scattering methods in which the muffin-tin spheres are replaced by space-filling atomic cells. The main change would consist in calculating the R-matrix for a sphere surrounding the atomic cell and where the potential in the so-called “moon-region” (the space outside the cell and inside the sphere) has been put to zero.

With the final state quantum numbers $\alpha\mathbf{k}s$, the sum in Eq. (17) becomes $\sum_{\alpha s} \int \frac{d\mathbf{k}^3}{8\pi^3}$. We have $\int \frac{d\mathbf{k}^3}{8\pi^3} = \frac{1}{16\pi^3} \int d\hat{\mathbf{k}} \int_0^\infty d\epsilon \sqrt{\epsilon}$, where $\epsilon = k^2$ is the kinetic energy of the photo-electron. This yields

$$\sigma = \frac{\alpha\omega}{4\pi} \sum_{\alpha s} k_\alpha \int d\hat{\mathbf{k}}_\alpha \left| \langle \Psi^{(\alpha\mathbf{k}_\alpha s)} | D | \Psi_g \rangle \right|^2,$$

where $k_\alpha^2 = E_g + \omega - E_\alpha$ from energy conservation. It is convenient to work in an angular momentum ba-

sis, i.e. to use spherical rather than plane waves. We have $\int d\hat{\mathbf{k}} |\mathbf{k}\rangle \langle \mathbf{k}| = 16\pi^2 \sum_L |kL\rangle \langle kL|$, where $\langle \mathbf{x} | kL \rangle = j_l(kr)Y_L(\hat{x}) \equiv J_L(k\mathbf{x})$. Here, j_l are the usual spherical Bessel functions and Y_L are spherical harmonics. The cross section now becomes

$$\sigma = 4\pi\alpha\omega \sum_{\alpha Ls} k_\alpha \left| \langle \Psi^{(\alpha Ls)} | D | \Psi_g \rangle \right|^2. \quad (18)$$

Here $\Psi^{(\alpha Ls)}$ is the scattering state that evolves from the incoming wave

$$\Psi^{\text{inc}} = \Phi_\alpha J_L(k_\alpha \mathbf{x}) \chi_s(\sigma). \quad (19)$$

Following standard multiple scattering theory, we write the scattered part of the wave as a sum of outgoing irregular waves from all the centers i

$$\Psi = \Psi^{\text{inc}} + \sum_i \Psi_i^{\text{sc}}$$

In the following we consider points where the photo-electron coordinate \mathbf{x} lies outside any muffin-tin sphere (or atomic cell). For such points the potential is zero and we have

$$\Psi_i^{\text{sc}} = -i \sum_{\alpha Ls} \Phi_\alpha k_\alpha H_L(k_\alpha \mathbf{x}_i) \chi_s(\sigma) B_{i\alpha Ls}^0. \quad (20)$$

Here $\mathbf{x}_i \equiv \mathbf{x} - \mathbf{R}_i$ and $H_L(k\mathbf{x}) \equiv h_l^+(kr)Y_L(\hat{x})$ where $h_l^+ = j_l + in_l$ is a Hankel and n_l a spherical Neumann function. As indicated by the superscript 0, the amplitudes $B_{i\alpha Ls}^0$ depend on the quantum numbers of Ψ^{inc} , which we shall denote $\alpha_0 L_0 s_0$ from now on. We use the well-known re-expansion theorems:

$$J_L(k\mathbf{x}_j) = \sum_{L'} J_{L'}(k\mathbf{x}_i) \Delta_{L'L}^{ij}(k) \quad (21)$$

$$-iH_L(k\mathbf{x}_j) = \sum_{L'} J_{L'}(k\mathbf{x}_i) G_{L'L}^{ij}(k) \quad (22)$$

where $\Delta_{L'L}^{ij}$ and $G_{L'L}^{ij}$ are the real space KKR structure constants.[14] Developing Ψ^{inc} and the Ψ_j^{sc} 's around some given center i and using equations (21) and (22), respectively, yields:

$$\Psi = \sum_{\alpha Ls} \Phi_\alpha \chi_s \left\{ J_L(k_\alpha \mathbf{x}_i) A_{i\alpha Ls}^0 - i k_\alpha H_L(k_\alpha \mathbf{x}_i) B_{i\alpha Ls}^0 \right\} \quad (23)$$

with

$$A_{i\alpha Ls}^0 = \delta_{\alpha\alpha_0} \delta_{s s_0} \Delta_{LL_0}^{i0}(k_\alpha) + k_\alpha \sum_{jL'} G_{LL'}^{ij}(k_\alpha) B_{j\alpha L's}^0, \quad (24)$$

where the usual convention $G_{LL'}^{ii} \equiv 0$ has been used.

Next we express the exciting wave amplitudes $A_{i\alpha Ls}^0$ in terms of the scattered wave amplitudes $B_{i\alpha Ls}^0$ at the same site i through the inverse atomic scattering matrices $(t_i^{-1})_{\alpha Ls, \alpha' L's'}$ as

$$A_{i\alpha Ls}^0 = \sum_{\alpha' L's'} (t_i^{-1})_{\alpha Ls, \alpha' L's'} B_{i\alpha' L's'}^0. \quad (25)$$

This holds by definition of the t_i -matrices, and relies only on the most basic assumption of multiple scattering theory, namely that the potential can be written as a sum of atomic cell potentials. Note that there is no restriction on the form of the atomic potentials, which may, as it is the case for the absorber potential in the present work, include non-local and correlation effects. (Note, however, that in the present approach the calculation of this complicated potential is avoided by virtue of the eigen-channel method.) Assuming the atomic t -matrices to be known, we may use Eq. (25) to eliminate the $A_{i\alpha Ls}^0$'s in Eq. (24), and then solve for the $B_{i\alpha Ls}^0$'s. This yields

$$B_{i\alpha Ls}^0 = \sum_{jL'} \tau_{\alpha Ls, \alpha_0 L' s_0}^{ij} \Delta_{L'L_0}^{j0}(k_{\alpha_0}) \quad (26)$$

where τ is the (multi-channel) scattering path operator which is defined by its matrix inverse:

$$(\tau^{-1})_{\Gamma\Gamma'}^{ij} \equiv \delta_{ij}(t_i^{-1})_{\Gamma\Gamma'} - \delta_{\alpha\alpha'} k_\alpha G_{LL'}^{ij}(k_\alpha) \delta_{ss'}, \quad (27)$$

where we have introduced the collective index $\Gamma \equiv \alpha Ls$. Equations (23–27) are the generalized multiple scattering equations.

We shall proceed by calculating the X-ray absorption cross section from an atom placed at the origin $\mathbf{R}_i = 0$. Using Eq. (25), the wave function in Eq. (23) around site $i = 0$ (index suppressed) reads

$$\Psi_{\Gamma_0} = \sum_{\Gamma\Gamma'} \tilde{\Phi}_\Gamma Z_{\Gamma\Gamma'}(r)/r B_{\Gamma'}^{\Gamma_0} \quad (28)$$

where

$$\tilde{\Phi}_\Gamma \equiv \Phi_\alpha Y_L(\hat{x}) \chi_s(\sigma) \quad (29)$$

and

$$Z_{\Gamma\Gamma'}(r)/r \equiv j_l(k_\alpha r)(t^{-1})_{\Gamma\Gamma'} - ik_\alpha h_l^+(k_\alpha r) \delta_{\Gamma\Gamma'}. \quad (30)$$

We recall that Eq. (23) or (28) is valid only in the space outside atomic spheres. For the region inside the atomic

sphere of the absorber, we may write

$$\Psi_{\Gamma_0} = \sum_{\Gamma} \Psi_\Gamma^{\text{in}} B_\Gamma^{\Gamma_0} \quad (31)$$

where Ψ_Γ^{in} is a solution of the Schrödinger equation inside the atomic sphere, that matches smoothly onto the outside wave function $\sum_{\Gamma'} \tilde{\Phi}_{\Gamma'} Z_{\Gamma'\Gamma}(r)/r$.

Putting this into the absorption cross section formula, Eq. (18), we obtain

$$\sigma = 4\pi\alpha\omega \sum_{\Gamma\Gamma'\Gamma_0} \langle \Psi_g | D^\dagger | \Psi_\Gamma^{\text{in}} \rangle k_{\Gamma_0} B_\Gamma^{\Gamma_0} B_{\Gamma'}^{\Gamma_0*} \langle \Psi_\Gamma^{\text{in}} | D | \Psi_g \rangle \quad (32)$$

Note that the restriction to Ψ^{in} in the calculation of the matrix elements is valid since we have assumed that Ψ_g vanishes outside the atomic cell. A further simplification of the formula can be achieved if we use the optical theorem, whose validity in the multi-channel case was proved in Ref. [1]:

$$\sum_{\Gamma_0} k_{\Gamma_0} B_{i\Gamma}^{\Gamma_0} B_{j\Gamma'}^{\Gamma_0*} = -\frac{1}{2i} (\tau - \tau^\dagger)_{\Gamma\Gamma'}^{ij} \quad (33)$$

If we moreover introduce the notation $M_\Gamma \equiv \langle \Psi_\Gamma^{\text{in}} | D | \Psi_g \rangle$ we finally obtain:

$$\sigma = -4\pi\alpha\omega \times \Im \left\{ \sum_{\Gamma\Gamma'} M_\Gamma^* \tau_{\Gamma\Gamma'}^{00} M_{\Gamma'} \right\} \quad (34)$$

In this form, the cross section formula reads exactly as the well-known one-particle expression (see e.g. Ref. [21]). The fundamental difference is that the quantum numbers Γ contain internal degrees of freedom of the absorbing atom (channels α), which in the present case correspond to different multi-electron states.

-
- [1] C. R. Natoli, M. Benfatto, C. Brouder, M. F. Ruiz Lopez, and D. L. Foulis, Phys. Rev. B **42**, 1944 (1990).
[2] W. Kohn, Phys. Rev. **74**, 1763 (1948).
[3] C. H. Greene, Phys. Rev. A **28**, 2209 (1983).
[4] H. Le Rouzo and G. Raseev, Phys. Rev. A **29**, 1214 (1984).
[5] P. Hamacher and J. Hinze, J. Phys. B **22**, 3397 (1989).
[6] M. Aymar, C. H. Greene, and E. Luc-Koenig, Rev. Mod. Phys. **68**, 1015 (1996).
[7] J. J. M. Michiels, J. E. Inglesfield, C. J. Noble, V. M. Burke, and P. G. Burke, Phys. Rev. Lett. **78**, 2851 (1997).
[8] M. W. D. Mansfield, Proc. R. Soc. Lond. A. **348**, 143 (1976).
[9] J. Zaanen, G. A. Sawatzky, J. Fink, W. Speier, and J. C. Fuggle, Phys. Rev. B **32**, 4905 (1985).
[10] F. M. F. de Groot, J. C. Fuggle, B. T. Thole, and G. A. Sawatzky, Phys. Rev. B **41**, 928 (1990).
[11] F. J. Himpsel, U. O. Karlsson, A. B. McLean, L. J. Terminello, F. M. F. de Groot, M. Abbate, J. C. Fuggle, J. A. Yarmoff, B. T. Thole, and G. A. Sawatzky, Phys. Rev. B **43**, 6899 (1991).
[12] J. Schwitalla and H. Ebert, Phys. Rev. Lett. **80**, 4586 (1998).
[13] A. L. Ankudinov, A. I. Nesvizhskii, and J. J. Rehr Phys. Rev. B **67**, 115120 (2003).
[14] For a definition of the structure constants, see e.g. Ref. [1] appendix A, where, however, they are denoted H and J rather than G and Δ , respectively.

- [15] We have used the *LAPACK* package, which is freely distributed at <http://www.netlib.org/lapack/>.
- [16] The transformation is given by $|2p^5\nu d^1, (LS)JM\rangle = \sum_{j_c\mu_c m_s} t_{LSJM, j_c\mu_c m_s} |2p^5 j_c\mu_c, \nu d^1 m_s\rangle$, where $t_{LSJM, j_c\mu_c m_s} = \sum_{M_L M_S m_c s_c} (LSM_L M_S | JM) \times (12m_c m | LM_L)(\frac{1}{2}\frac{1}{2}s_c s | SM_S)(1\frac{1}{2}m_c s_c | j_c\mu_c)$ and $(\dots|\dots)$ are Clebsch-Gordan coefficients.
- [17] E. U. Condon, G. H. Shortley, *The Theory of Atomic Spectra*, Cambridge University Press, Cambridge, England, 1951, ch. 1¹³, p. 299, table for $(p^5 d^1)$ configuration.
- [18] R. D. Cowan, *The Theory of Atomic Structure and Spectra* (University of California Press, Berkeley, 1981), p. 464, and references therein.
- [19] C. R. Natoli, D. K. Misemer, S. Doniach, and F. W. Kutzler, Phys. Rev. A **22**, 1104 (1980).
- [20] O. K. Andersen and O. Jepsen, Phys. Rev. Lett. **53**, 2571 (1984).
- [21] D. D. Vvedensky, in *Unoccupied Electronic States*, J. C. Fuggle and J. E. Inglesfield, Eds, Springer-Verlag, Berlin, Heidelberg, 1992, chapter 5.